

Inspection of subsurface defects in the composite materials by divergence-based analysis over the phase velocity vector field

Kenbu Teramoto
Dept. of Mechanical Engineering
Saga University
Saga, Japan
tera@cc.saga-u.ac.jp

Haruka Ishibashi
Dept. of Advanced Technology Fusion
Saga University
Saga, Japan
terremotolab@gmail.com

Abstract—In recent decades, CFRP materials have been extensively used in engineering process and become an important material in many industries. Ultrasonic guided waves, Lamb waves, are useful for evaluating the integrity of CFRP structures. However, the variation of the Lamb wave velocity causes difficulties for interpretation of observed signals. It is important, therefore, to establish the crack detection criterion independent of wave numbers. The aim of this work is to retrieve divergence of the phase velocity vector field caused by the scattered waves and to reconstruct the image of sub-surface defects. In this study, the problem of reconstructing a super-resolved image of defects in a shell structures over Lamb wave field is considered. This study discusses the image reconstruction process based on the divergence of the phase velocity vector field of the scattered wave fronts.

Index Terms—divergence based sensing, structural health monitoring, guided wave, composite material, ultrasonic testing

I. INTRODUCTION

In many decades, guided waves have been used for non-destructive evaluation. In 1967, Viktorov described a flaw detection by using of Rayleigh and Lamb waves. From then, guided wave ultrasonic testing (GWUT) methods have been considered as fast-screening techniques to inspect long distances of a structure [1]. Hayashi and Kawashima studied the reflection characteristics of S0 and A0-mode Lamb waves and showed that the A0-mode Lamb wave is sensitive to the delamination at all through-thickness locations [2]. In addition, because the A0-mode Lamb wave has shorter wavelength than S0-mode Lamb wave at the same frequency, it is potentially more sensitive to delamination damage. Due to the above reason, A0-mode Lamb waves measurement has been utilized as one of the promising structural health monitoring techniques for detecting hidden damage in composites [3]–[5]. The Glushkovs show the influence of anisotropy and lamination on forced wave energy radiation and its spatial directivity and modal partitioning based on the integral approach [6]. However, the variation of phase velocity causes difficulties for interpretation of observed signals. It is important, therefore, to establish the crack detection and imaging criterion independent

of local wave numbers [7]–[9]. In this study, the problem of reconstructing a silhouette of defects in the thin-plate-like structures over A0-mode Lamb-wave field is considered. Focusing on the divergences of the phase velocity vector field of the wave front which is scattered by the subsurface defect in the CFRP plate, the proposed algorithm is summarized as follows:

- 1) obtaining out-of-surface displacements and the orthogonal pair of out-of-surface shear strains,
- 2) calculating cross-correlations between the above strains and the normal displacement,
- 3) reconstructing divergence of the phase velocity vector field with dividing the above sum of squares by the square of the auto-correlation of the normal displacements.

II. PROBLEM FORMULATION

Being focused on the fundamental order antisymmetric Lamb wave (A0-mode Lamb wave) propagating over the quasi-isotropic CFRP plate, the vertical displacement can be approximated to be governed by the 2-dimensional wave equation. In the region without sound sources, the A0-mode Lamb-wave field is governed by the following wave equation:

$$\nabla^2 u(\mathbf{r}, t) - \frac{1}{\|\mathbf{c}(\mathbf{r})\|^2} \frac{\partial^2}{\partial t^2} u(\mathbf{r}, t) = 0 \quad (1)$$

where, \mathbf{r} , t , $u(\mathbf{r}, t)$ and $\mathbf{c}(\mathbf{r})$ denote the location vector on the surface, time, the out-of-surface displacement, and the phase velocity vector of the A0-mode Lamb-wave respectively. Using 2-dimensional cylindrical coordinates, the above differential equation can be denoted as:

$$\left(\frac{\partial^2}{\partial r^2} + \frac{1}{r} \frac{\partial}{\partial r} + \frac{1}{r^2} \frac{\partial^2}{\partial \phi^2} - \frac{1}{c^2} \frac{\partial^2}{\partial t^2} \right) u(\mathbf{r}, t) = 0. \quad (2)$$

When a single point source exists on the origin, a wave equation with only cylindrically symmetric solutions is expressed as:

$$\frac{\partial u(\mathbf{r}, t)}{\partial \phi} = 0. \quad (3)$$

Consequently, the differential equation

$$\left(\frac{\partial^2}{\partial r^2} + \frac{1}{r} \frac{\partial}{\partial r} - \frac{1}{c^2} \frac{\partial^2}{\partial t^2}\right)u(\mathbf{r}, t) = 0 \quad (4)$$

can be obtained. Using the following relation

$$\frac{\partial^2}{\partial r^2} + \frac{1}{r} \frac{\partial}{\partial r} \rightarrow \left(\frac{\partial}{\partial r} + \frac{1}{2r}\right)\left(\frac{\partial}{\partial r} + \frac{1}{2r}\right),$$

the above 2nd order differential equation, (4), can be factorized as [10]:

$$\begin{aligned} &\left(\frac{\partial^2}{\partial r^2} + \frac{1}{r} \frac{\partial}{\partial r} - \frac{1}{c^2} \frac{\partial^2}{\partial t^2}\right)u(\mathbf{r}, t) \\ &= \left(\frac{\partial}{\partial r} + \frac{1}{2r} + \frac{1}{c} \frac{\partial}{\partial t}\right)\left(\frac{\partial}{\partial r} + \frac{1}{2r} - \frac{1}{c} \frac{\partial}{\partial t}\right)u(\mathbf{r}, t) \\ &= 0. \end{aligned} \quad (5)$$

Considering the divergent wave fronts, the following 1st order differential equation,

$$\left(\frac{\partial}{\partial r} + \frac{1}{2r} + \frac{1}{c} \frac{\partial}{\partial t}\right)u(\mathbf{r}, t) = 0 \quad (6)$$

is satisfied. Consequently, the equivalent vector differential equations can be obtained as follows:

$$\nabla u(\mathbf{r}, t) = -\frac{\mathbf{r}}{c\|\mathbf{r}\|} \left(\frac{\partial u(\mathbf{r}, t)}{\partial t} + \frac{1}{2r}c u(\mathbf{r}, t)\right) \quad (7)$$

When the point source exists on \mathbf{r}_0 , the above differential equation is changed to be:

$$\nabla u(\mathbf{r}, t) = -\frac{\mathbf{r} - \mathbf{r}_0}{c\|\mathbf{r} - \mathbf{r}_0\|} \left(\frac{\partial u(\mathbf{r}, t)}{\partial t} + \frac{1}{2\|\mathbf{r} - \mathbf{r}_0\|}c u(\mathbf{r}, t)\right). \quad (8)$$

The phase velocity vector field of the cylindrical wave diverging from the source, \mathbf{r}_0 , can be denoted as:

$$\mathbf{c}(\mathbf{r}) = c \cdot \frac{\mathbf{r} - \mathbf{r}_0}{\|\mathbf{r} - \mathbf{r}_0\|}. \quad (9)$$

Consequently, the divergence of the phase velocity vector field can be obtained as:

$$\nabla \cdot \mathbf{c}(\mathbf{r}) = \frac{c}{\|\mathbf{r} - \mathbf{r}_0\|}. \quad (10)$$

Substituting eq.(10) into eq.(8), the following vector differential equations is derived:

$$\begin{aligned} \nabla u(\mathbf{r}, t) &= -\frac{\mathbf{c}(\mathbf{r})}{\|\mathbf{c}(\mathbf{r})\|^2} \\ &\cdot \left(\frac{\partial u(\mathbf{r}, t)}{\partial t} + \frac{1}{2}(\nabla \cdot \mathbf{c}(\mathbf{r}))u(\mathbf{r}, t)\right). \end{aligned} \quad (11)$$

In order to exclude the term of temporal derivatives, the cross correlations between the surface displacement and its corresponding gradient vector are introduced as follows:

$$\begin{aligned} \Phi_{ru}(\mathbf{r}) &= \lim_{T \rightarrow \infty} \frac{1}{T} \int_{-T/2}^{T/2} \frac{\partial u(\mathbf{r}, t)}{\partial r} u(\mathbf{r}, t) dt \\ &= -\frac{c_r(\mathbf{r})}{2\|\mathbf{c}(\mathbf{r})\|^2} \nabla \cdot \mathbf{c}(\mathbf{r}) \Phi_{uu}(\mathbf{r}) \end{aligned} \quad (12)$$

$$\begin{aligned} \Phi_{\phi u}(\mathbf{r}) &= \lim_{T \rightarrow \infty} \frac{1}{T} \int_{-T/2}^{T/2} \frac{1}{r} \frac{\partial u(\mathbf{r}, t)}{\partial \phi} u(\mathbf{r}, t) dt \\ &= -\frac{c_\phi(\mathbf{r})}{2\|\mathbf{c}(\mathbf{r})\|^2} \nabla \cdot \mathbf{c}(\mathbf{r}) \Phi_{uu}(\mathbf{r}) \end{aligned} \quad (13)$$

Here, the auto-correlation $\Phi_{uu}(\mathbf{r})$ can be defined as:

$$\Phi_{uu}(\mathbf{r}) = \lim_{T \rightarrow \infty} \frac{1}{T} \int_{-T/2}^{T/2} u(\mathbf{r}, t) u^*(\mathbf{r}, t) dt, \quad (14)$$

and the following relation:

$$0 = \lim_{T \rightarrow \infty} \frac{1}{T} \int_{-T/2}^{T/2} \frac{\partial u(\mathbf{r}, t)}{\partial t} u^*(\mathbf{r}, t) dt, \quad (15)$$

is utilized. Based on the above discussion, the following relation is derived,

$$\frac{\Phi_{ru}^2(\mathbf{r}) + \Phi_{\phi u}^2(\mathbf{r})}{\Phi_{uu}^2(\mathbf{r})} = \frac{1}{4\|\mathbf{c}(\mathbf{r})\|^2} (\nabla \cdot \mathbf{c}(\mathbf{r}))^2 \quad (16)$$

In the case of isotropic material, $\|\mathbf{c}(\mathbf{r})\|$ becomes constant everywhere, therefore the ratio between $|\Phi_{xu}(\mathbf{r})|^2 + |\Phi_{yu}(\mathbf{r})|^2$ and $\Phi_{uu}^2(\mathbf{r})$ is proportional to the divergence of the phase velocity vector field. The equation (16) shows the principle of the newly proposed divergence based analysis.

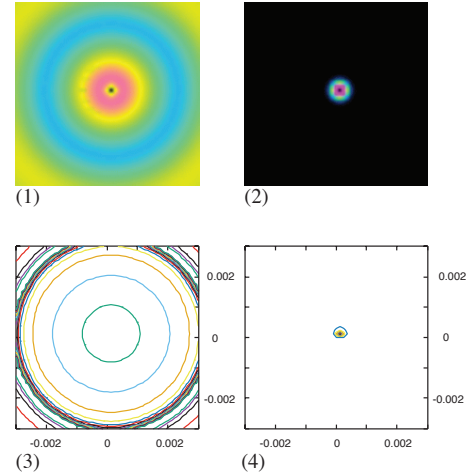


Fig. 1. (1) A cylindrical wave front spreading from the single point source, (2) reconstructed image of the point source obtained by the left side value of eq.(16), (3) iso-phase plot of the above cylindrical wave front, (4) the image of divergence of the phase velocity vector field.

III. ACOUSTICAL EXPERIMENTS

This section presents an experimental verification of the proposed detecting method described in Sec. II.

A. Proof-Of-Concept Model

Figure 2(1) shows the external view of the micro laser interferometer which detects the out-of-plane displacement. The foot print of the laser beam is shown in Fig.2(2). Fig.2(3) shows the block diagram of the proof-of-concept model. Normal displacements of the plate are observed by the *Michelson* interferometric probe (a) which can detect 0.08nm

in amplitude. Single transmitter(b) is located at the center of the specimen and radiates 29kHz-mono-cycle cylindrical wave. A composite laminate specimen,(c), with 2.3mm in thickness is provided for the measurement. The inspected area is covered by an aluminum film with 12 μ m in thickness.

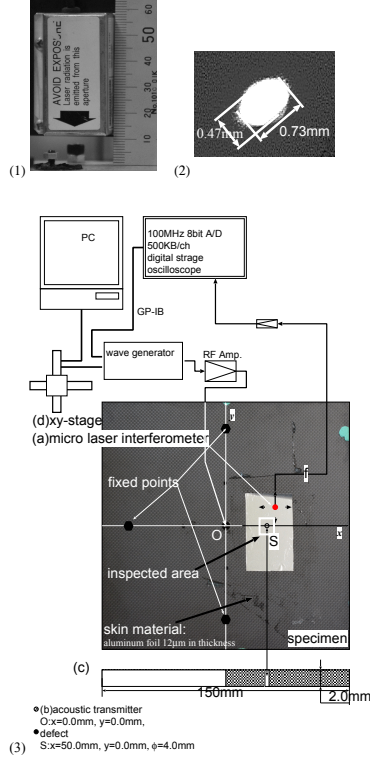


Fig. 2. (1)A view of the micro laser interferometer (MLI-80), (2)A foot print of the probing laser beam, and (3)block diagram of the proof of concept model and its geometrical relationship with a specimen for inspection. The inspected area is covered by the aluminum film which is 12 μ m in thickness.

Figure 3 illustrates the proposed detecting method based on the divergence of the phase-velocity vector field. The out-of-plane strains, are obtained by horizontal and vertical Sobel-filtering as:

$$\frac{\partial u(\mathbf{r}, t)}{\partial x} \triangleq \sum_{\xi=-2}^2 \sum_{\zeta=-2}^2 S_{obelx}^{[5 \times 5]}(\xi, \zeta) \cdot u(x - \xi \Delta x, y - \zeta \Delta y, t) \quad (17)$$

$$\frac{\partial u(\mathbf{r}, t)}{\partial y} \triangleq \sum_{\xi=-2}^2 \sum_{\zeta=-2}^2 S_{obely}^{[5 \times 5]}(\xi, \zeta) \cdot u(x - \xi \Delta x, y - \zeta \Delta y, t) \quad (18)$$

Here, Δt , Δx , and Δy are the sampling interval time (=10ns), x and y directional the sampling interval (=0.125mm) respectively. Figure 3 illustrates the imaging process of the proposed detecting method.

The cross correlations between the out-of-surface displacement signal and the corresponding orthogonal pair of gradient

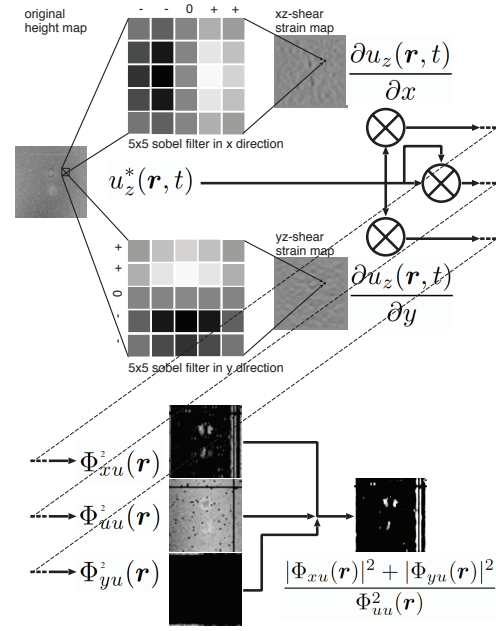


Fig. 3. Image reconstruction process utilizing cross correlations between the out-of-surface displacement signal and the corresponding orthogonal pair of gradient signals

signals are derived from the following summation of the decaying serieses [11]–[13]:

$$\Phi_{xu} = \frac{1}{N \Delta t} \sum_{n=0}^N \alpha^n \cdot \frac{\partial u(\mathbf{r}, (N-n)\Delta t)}{\partial x} \cdot u(\mathbf{r}, (N-n)\Delta t) \Delta t, \quad (19)$$

$$\Phi_{yu} = \frac{1}{N \Delta t} \sum_{n=0}^N \alpha^n \cdot \frac{\partial u(\mathbf{r}, (N-n)\Delta t)}{\partial y} \cdot u(\mathbf{r}, (N-n)\Delta t) \Delta t, \quad (20)$$

where α satisfies the time constant $\tau = 50\mu$ s as:

$$\alpha = e^{-\Delta t / \tau} \quad (21)$$

The time-constant, τ , should be much longer than the period of the incident wave, because the integral duration is controlled by τ .

B. Defect imaging based on the divergence of the phase velocity vector field

1) *Isotropic material case:* Figure 4(1) shows the geometrical sketch of the cylindrical through-hole, which is covered with aluminum film 12 μ m in thickness. The aluminum film is adhered to the surface of S45C plate except the circular region. Figure 4(2) shows the snap shot distributions of the normalized vertical particle displacement. The corresponding, Fig.4(3) shows the image which is reconstructed by the newly proposed method based on the divergence of the phase velocity vector.

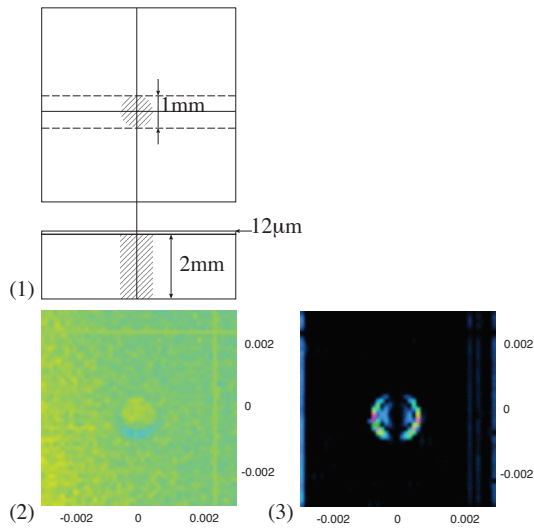


Fig. 4. (1) A geometrical sketch of a cylindrical through-hole of which diameter is 1mm, (2) the distributions of the normalized vertical particle displacement, (3) reconstructed image of the through-hole defect obtained by the left side value of eq. (16).

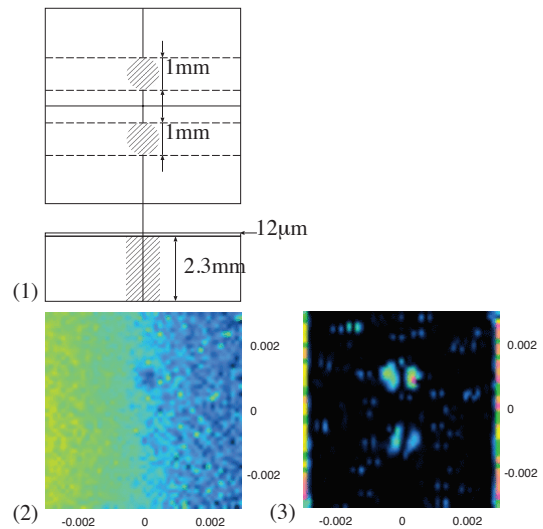


Fig. 6. (1) A geometrical sketch of a cylindrical through-holes of which diameter is 1mm, (2) the distributions of the normalized vertical particle displacement, (3) reconstructed image of the through-hole defect obtained by the left side value of eq. (16).

2) *orthotropic material case*: A CFRP plate has orthotropy on linear elasticity. The phase velocity of the A0-mode Lamb wave varies in the azimuthal angles, therefore, the divergent wave front can be observed shown in Fig.5. Figures 6(1), (2),

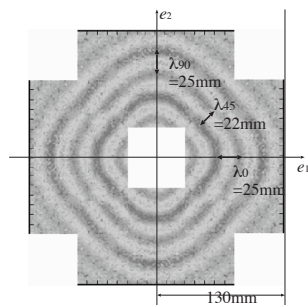


Fig. 5. A divergent wavefront of A0mode Lamb-wave propagating over the CFRP plate

and (3) are obtained by the same way of the above isotropic case.

IV. CONCLUDING REMARKS

This study can be summarized as follows:

- 1) a novel non-destructive inspection method based on the divergence of the phase velocity vector field is proposed and evaluated mathematically in isotropic material case.
- 2) several acoustical experiments show the feasibility of the proposed method.
- 3) the advantages of the divergence based method are shown by comparison with the dynamic shear strain analysis.

REFERENCES

[1] I.A.Viktorov, "Rayleigh and Lamb Waves," Springer US, 1967

[2] T.Hayashi, K.Kawashima, "Multiple reflections of Lamb waves at a delamination", Ultrasonics, vol.40, pp. 193–197, 2002

[3] C.Prada, O.Balogun and T.W.Murray, "Laser-based ultrasonic generation and detection of zero-group velocity Lamb waves in thin plates," Appl.Phys.Lett. vol.87, p.194109, 1/3, 2005

[4] J.Laurent, D.Royer, T.Hussain, F.Ahmad, C.Prada, "Laser induced zero-group velocity resonances in transversely isotropic cylinder," The Journal of the Acoustical Society of America, vol.137-6, pp. 3325–3334, 2015

[5] A.Velichko, P.D.Wilcox, "Modeling the excitation of guided waves in generally anisotropic multilayered media", The Journal of the Acoustical Society of America, vol.121-1, pp. 60–69, 2007

[6] E. Glushkov, N. Glushkova, and A. Eremin, "Forced wave propagation and energy distribution in anisotropic laminate composites", The Journal of the Acoustical Society of America, vol. 129-5, pp. 2923-2934, 2011

[7] K.Teramoto, K.Tsuruta, "Non-destructive Testing Based on the Spatio-temporal Gradient Analysis over the Lamb Wave Field," Transactions of the Society of Instrument and Control Engineers, vol. 39-9, pp. 800–807, 2003

[8] K.Teramoto, R.Inoue, "Near-field Imaging of Defects Based on the Dynamic Shear Strain Analysis over the A0-mode Lamb Wave Field," Transactions of the Society of Instrument and Control Engineers, vol.47-10, pp. 422–429, 2011

[9] K.Teramoto, K.Tsuruta, "Spatio-Temporal Gradient Analysis for Detecting Defects (in Japanese)," IEICE TRANS. FUNDAMENTALS, vol.87A-8, pp. 2037–2044, 2004

[10] S.Ando, T.Nara, T.Levy, "Partial differential equation-based localization of a monopole source from a circular array (in Japanese)," The Journal of the Acoustical Society of America, vol.134-4, pp. 2799–2813, 2013

[11] S.Ando, N.Ono, "Partial differential equation (PDE)-based theory of sound source localization," 4th Joint Meeting ASA/ASJ, Honolulu, Hawaii, 2006

[12] S.Koyama, T.Kurihara, S.Ando, "A Theory and Experiment of Instantaneous Wave Source Localization from a Wave Distribution on a Small Region," IEEE Transactions on Sensors and Micromachines, vol.129-10, pp. 350–356, 2009

[13] S.Ando, H.Shinoda, K.Ogawa, S.Mitsuyama, "A Three-Dimensional Sound Localization Sensor System Based on the Spatio-Temporal Gradient Method (in Japanese)," Transactions of the Society of Instrument and Control Engineers, vol.29-5, pp. 520–528, 1993